

Membrane Biophysics

Altered Membrane Mechanics Provides a Receptor-Independent Pathway for Serotonin Action

Simli Dey,^[a] Dayana Surendran,^[a] Oskar Engberg,^[b] Ankur Gupta,^[a] Sashaina E. Fanibunda,^[c, d] Anirban Das,^[a] Barun Kumar Maity,^[a] Arpan Dey,^[a] Vicky Visvakarma,^[a] Mamata Kallianpur,^[a] Holger A. Scheidt,^[b] Gilbert Walker,^[e] Vidita A. Vaidya,^[c] Daniel Huster,^{*,[a, b]} and Sudipta Maiti^{*,[a]}

Abstract: Serotonin, an important signaling molecule in humans, has an unexpectedly high lipid membrane affinity. The significance of this finding has evoked considerable speculation. Here we show that membrane binding by serotonin can directly modulate membrane properties and cellular function, providing an activity pathway completely independent of serotonin receptors. Atomic force microscopy shows that serotonin makes artificial lipid bilayers softer, and induces nucleation of liquid disordered domains inside the raft-like liquid-ordered domains. Solid-state NMR spectroscopy

corroborates this data at the atomic level, revealing a homogeneous decrease in the order parameter of the lipid chains in the presence of serotonin. In the RN46A immortalized serotonergic neuronal cell line, extracellular serotonin enhances transferrin receptor endocytosis, even in the presence of broad-spectrum serotonin receptor and transporter inhibitors. Similarly, it increases the membrane binding and internalization of oligomeric peptides. Our results uncover a mode of serotonin–membrane interaction that can potentiate key cellular processes in a receptor-independent fashion.

Introduction

The neurotransmitter serotonin, in addition to its directed action through synaptic signalling, has an indirect neuro-modulatory role.^[1–6] A significant amount of serotonin is released from extra-synaptic areas, including from the cell body, away from the site of post-synaptic receptor densities.^[7–11] Even when they are released at the synapses, a large fraction diffuses away from the synaptic cleft.^[12] This temporally and spatially diffuse “volume neurotransmission”^[8,9,13–15] appears to be a somewhat wasteful attempt to reach far-away targets. However, a recent discovery of the high affinity of serotonin for lipid bilayers^[16,17] suggests that the lipid membrane may be a ubiquitously present target for such release. Indeed, it has been

speculated that attachment and two-dimensional diffusion of serotonin in the lipid membrane may facilitate distal receptor binding.^[18,19] Here, we hypothesize and demonstrate that passive serotonin-membrane interaction can give rise to an entirely receptor-independent pathway for modulating specific cell functions. This pathway is mediated through a modulation of the mechanical properties of the membrane.

Cholesterol is a classic example of a molecule altering the mechanical properties of the membrane, with very significant biological consequences. It has been recently shown that cholesterol can change the bending rigidity of both the ordered and disordered regions of a lipid bilayer membrane.^[20] Small amphipathic molecules, for example, specific anesthetics, are known to alter the physical properties of the membrane, such


[a] Dr. S. Dey, Dr. D. Surendran, A. Gupta, A. Das, Dr. B. K. Maity, A. Dey, V. Visvakarma, M. Kallianpur, Prof. Dr. D. Huster, Prof. Dr. S. Maiti
Department of Chemical Sciences
Tata Institute of Fundamental Research
Homi Bhabha Road, Colaba, Mumbai 400005 (India)
E-mail: maiti@tifr.res.in


[b] Dr. O. Engberg, Dr. H. A. Scheidt, Prof. Dr. D. Huster
Institute of Medical Physics and Biophysics
University of Leipzig
Härtelstr. 16–18, 04107 Leipzig (Germany)
E-mail: daniel.huster@medizin.uni-leipzig.de

[c] Dr. S. E. Fanibunda, Prof. Dr. V. A. Vaidya
Department of Biological Sciences
Tata Institute of Fundamental Research
Homi Bhabha Road, Colaba, Mumbai 400005 (India)

[d] Dr. S. E. Fanibunda
Kasturba Health Society
Medical Research Center
Mumbai (India)

[e] Prof. Dr. G. Walker
Department of Chemistry
University of Toronto
Toronto, Ontario M5S3H6 (Canada)

 Supporting information and the ORCID identification numbers for the authors of this article can be found under:
<https://doi.org/10.1002/chem.202100328>.

 © 2021 The Authors. Chemistry - A European Journal published by Wiley-VCH GmbH. This is an open access article under the terms of the Creative Commons Attribution Non-Commercial NoDerivs License, which permits use and distribution in any medium, provided the original work is properly cited, the use is non-commercial and no modifications or adaptations are made.

as membrane fluidity.^[21–25] It has also been shown that isothermal compressibility of lipid monolayers can be altered by small serotonin-related molecules (such as melatonin) at ≈ 1 mM concentration, and even by serotonin at higher concentrations.^[26] Furthermore, serotonin binding to raft-like mixed model membranes was shown to alter domain size.^[27,28] If serotonin also changes the mechanical properties of the bilayer, then that in turn can affect cellular functions, including membrane protein function, membrane affinity of other molecules as a prerequisite for subsequent receptor binding, and key cellular processes such as exocytosis and endocytosis.

In this work, we set out to resolve an important question: do receptor independent changes of the physical properties of the membrane, induced by local serotonin concentrations, affect the cellular response? We used a broad array of biophysical tools to probe whether binding of serotonin affects membrane mechanical properties and the degree of local molecular order. We then examine the effect of such modulation on live cells. We probe membrane binding by proteins known to be co-secreted with serotonin and also measure the rate of constitutive endocytosis. We show that passive binding of serotonin to the membrane does indeed modulate cellular function independent of the receptors, uncovering a novel manner in which this neurotransmitter can also influence biological function.

Results

Effect of serotonin on mono- and biphasic lipid bilayers

Serotonin interacts with model lipid membranes

We measure the binding of serotonin to small unilamellar lipid vesicles (SUVs) of two different lipid compositions: a zwitterionic mix of DOPC (1,2-dioleoyl-*sn*-glycero-3-phosphocholine): egg sphingomyelin: cholesterol, molar ratio 2:2:1 (DEC221), and a negatively charged mix of POPC (1-palmitoyl-2-oleoyl-*sn*-glycero-3-phosphocholine): PPG (1-palmitoyl-2-oleoyl-*sn*-glycero-3-phospho-*rac*-(1'-glycerol) : cholesterol, molar ratio 1:1:1 (PPC111). We note that the identity of the lipids and membrane electrostatics appears to be important for serotonin binding.^[16,17] We test the degree of membrane-binding of serotonin using a dialysis retention assay described earlier.^[29] Both SUV dispersions of PPC111 and DEC221 at 2.5 mg mL^{-1} were incubated with 4.1 mM serotonin for 1 h, and then dialyzed against deionized water using a 100 kDa molecular weight cut off (MWCO) membrane permeable for serotonin (but not for the SUVs) for 18 hrs. Vesicle-bound serotonin would not diffuse out of the dialysis tubing, but free serotonin would. A control sample contains only 4.1 mM serotonin (no SUVs). Fluorescence signal (excitation 270 nm, emission 300–500 nm) from the dialyzed solution yields the concentration of the serotonin remaining in the dialysis tube. Excess serotonin fluorescence compared to the control sample provides the amount of membrane-attached serotonin (supplementary Figure S1A). The concentration of serotonin remaining after dialysis is determined from a calibration curve obtained from known concentrations of serotonin (supplementary Figure S1B). We observe

that 0.24% of serotonin remains in the DEC221 solution, 3.53% is retained in the PPC111 solution, and only a trace amount ($\approx 0.005\%$) is retained in the solution without vesicles. This implies that serotonin binds strongly to the lipid membrane, and binding was dependent on the lipid charge. Assuming no lipid losses during the whole process, the partition coefficient of serotonin is calculated to be 90 and 1500 in DEC221 and PPC111, respectively. This is in reasonable agreement with the reported values.^[16]

We used fluorescence microscopy to verify whether serotonin also binds to supported lipid bilayers (SLB). Serotonin can be visualized directly using three-photon microscopy,^[30] or by using conventional fluorescence microscopy with a fluorogenic compound. The effectiveness of OPA (*ortho*-phthalaldehyde) in fluorogenically detecting serotonin was demonstrated recently.^[31] At room temperature, the DEC221 bilayer exhibits two different coexisting phases.^[32] The phase enriched with SM and cholesterol is more ordered and is known as the Liquid Ordered (L_o) phase.^[33] The other phase is more disordered and is dominated by DOPC known as the Liquid Disordered (L_d) phase. A $100 \mu\text{M}$ serotonin solution is incubated with biphasic SLBs of DEC 221, which are characterized by the co-existence of L_o and L_d domains for 30 minutes and then washed with water to remove unbound serotonin. $100 \mu\text{M}$ of OPA is then added to this SLB and incubated further for 30 mins. The sample is imaged in a confocal microscope (excitation at 488 nm, and collection from 500 to 650 nm, see supplementary Figure S2B). The fluorescence image of a control solution, identical in all respects except that serotonin is absent, is shown in supplementary Figure S2A. The image clearly shows that serotonin strongly binds to the SLB. It is apparent from the image that serotonin preferably binds to the disordered domain (also confirmed by simultaneous AFM-confocal microscopy measurement) compared to the ordered domain (supplementary Figure S2D,E). The ratio of serotonin bound to the disordered vs. the ordered domain is approximately 4 (supplementary Figure S2C). We next ask the question: does serotonin binding promote disorder and induce the formation of the disordered domains?

Serotonin binding reduces the force of indentation in membranes

We perform AFM measurements on the SLBs to probe whether serotonin binding has an effect on the mechanical properties of the membrane. We measure membrane stiffness by determining the force of indentation, i.e., the force needed to rupture the bilayer (a representative force curve is shown in Figure 1A with an arrow marking the point of indentation). In the rest of this manuscript, “stiffness” implies the force of indentation. This is first determined in water in the absence of serotonin, and again after incubating the same bilayer with 4.1 mM serotonin for 60 min. For the monophasic PPC111 bilayer, the results are presented as a histogram (Figure 1B, $n = 1410$ force curves), and the average force is shown in Figure 1C. Serotonin reduces the indentation force by $58 \pm 19\%$. As a control experiment, we perform similar measurements in the absence and in

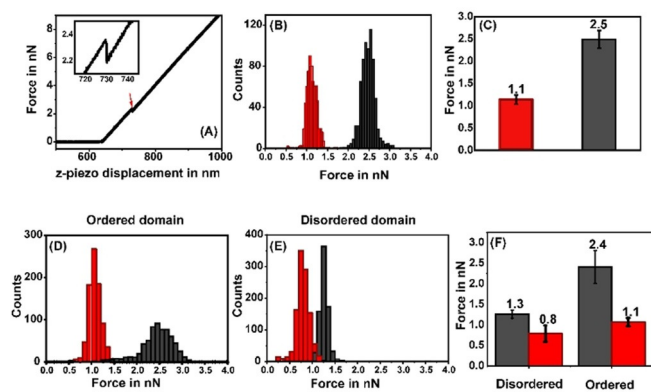


Figure 1. Probing the stiffness of membrane lipid bilayers by AFM force-indentation measurements. (A) A typical indentation force curve obtained from supported POPC/POPG/cholesterol (1:1:1) lipid bilayer on mica. The force applied by the cantilever is plotted as a function of the z-piezo displacement. The discontinuity in the force curve marks the point of indentation (red arrow). Inset: magnified image shows an indentation force of 2.2 nN. (B) Representative histogram of indentation forces before (black) and after (red) serotonin incubation on a negatively charged (PPC111) bilayer. (C) Average values of force histograms. (D), (E) representative histograms of indentation forces measured on the ordered and disordered domains, respectively on a neutral biphasic (DEC221) bilayer. (F) Average values of force histograms before (black) and after (red) serotonin incubation.

the presence of 4.1 mM glutamate, an excitatory neurotransmitter (supplementary Figure S3). In contrast to the effect of serotonin, glutamate does not cause any observable alterations in the force of indentation. It is likely that the charged glutamate molecule does not even attach to the lipid membrane, but it shows that not all neurotransmitters change membrane properties. The pH inside an intracellular neurotransmitter vesicle is about 5.5, while that on the plasma membrane is 7.4. We also tested whether serotonin could change the pH of the solution and whether just a change of pH could affect the force of indentation. We found these effects to be minimal, as described in supporting Figures S4 and S5.

Local membrane order and lateral organization can be an important parameters determining cell signaling, and so we probe the effect of serotonin on the phase separation of lipid bilayers. Sphingomyelin and cholesterol are frequently involved in creating local membrane domains.^[34] AFM imaging characterizes the co-existence of the two phases in the DEC221 bilayer (as described in methods). We obtain ordered lipid domains with diameters on the order of a few μm . The height difference between L_o and L_d matches well with the previously reported values (from ≈ 0.8 nm to 1.0 nm^[35]). For indentation measurements on this biphasic bilayer, we first map the individual L_o and L_d domains and then collect traces from the AFM images. The resulting histograms are shown in Figure 1D (for ordered domains) and Figure 1E (disordered domains). The resulting force distribution is shown in Figure 1F. We see that in the absence of serotonin, the L_o domains in the bilayer are stiffer (i.e. the indentation force is higher) compared to the L_d domains, as is expected. In the presence of serotonin, the force of indentation decreases in both the domains, but the decrease is much higher for the ordered domains. The force in the L_o domain decreases by $52.0 \pm 8.3\%$ while that in

the L_d domain decreases by $32.0 \pm 10.3\%$ ($n=5508$ force curves from 2 different bilayers).

Serotonin shrinks ordered domains in phase-separated bilayers

Biological cell membranes display a transient domain structure that is believed to play a major role in protein trafficking, in the interaction of the membrane with the cytoskeleton, and in cell signalling.^[36–38] Our observation that the indentation force of the L_o domains of DEC221 decreases drastically may suggest that serotonin can have an effect on the relative stability of the ordered and disordered domains. We characterized the area and the perimeter of the L_o and L_d domains before and after incubation with serotonin. We observe that serotonin induces nucleation of disordered domains within the ordered domains (Figure 2, see insets, which show magnified images of a representative area marked with dashed borders in the main Figure). There is an overall decrease of the area of the ordered domain. A control sample shows no such changes over the same amount of time (supplementary Figure S6). We also obtain a measure of the surface tension at the domain interface. The area of the interface between two domains is equal to the perimeter times the thickness of the bilayer, while the volume is given by the lateral area times the thickness. Since a higher surface tension implies smaller interface area per unit volume, the ratio of these two quantities, that is, the perimeter divided by the lateral area, provides a measure of the surface tension.

We find that the surface tension decreases by $34.0 \pm 2.1\%$ in the presence of serotonin ($n=133$). A lower surface tension is consistent with the decrease of the force of indentation found earlier.

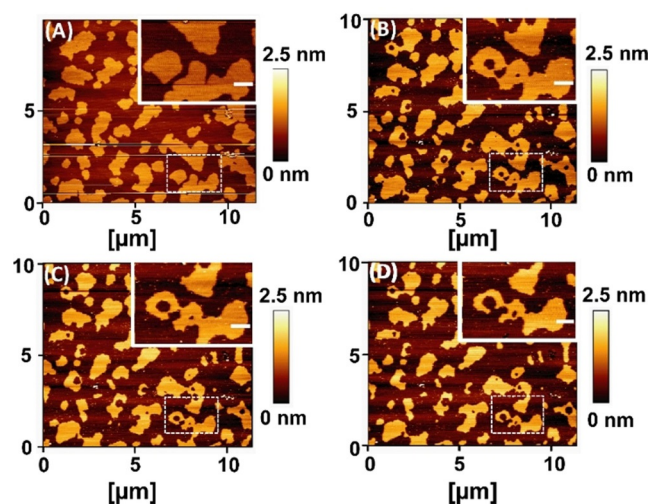


Figure 2. AFM images displaying time-dependent nucleation of disordered domains within the ordered domains in phase separated lipid bilayers (DEC221) (A) 0 min (B) 20 min, (C) 120 min, and (D) 300 min after incubation with 4.1 mM of serotonin. Insets: magnified images of the region with white dashed border, showing growth of disordered domain inside ordered domains. Scale bar 0.5 μm . Height is false color coded. Color bar indicates the relative height.

Serotonin promotes lipid chain disorder

Solid-state NMR can probe the molecular order along lipid chains. ^2H NMR has an intrinsic timescale on the order of $10\ \mu\text{s}$ allowing to detect spatial lipid heterogeneities with a radius larger than $\approx 25\ \text{nm}$ due to lipid translational exchange and diffusion.^[39–41] We perform solid-state NMR experiments on multilamellar PPC111 vesicles containing serotonin and determine the order parameters of the lipid protons. We record the ^2H NMR spectra of either deuterated POPC- d_{31} or POPG- d_{31} in the mixture in the presence of 0, 10, and 25 mol% serotonin (supplementary Figure S7). From the NMR spectra, order parameter plots for each deuterated lipid at 25 and 37 °C are determined and are shown in supplementary Figure S8. We observe that in the presence of serotonin, lipid chain order is homogeneously decreased along the entire *sn*-1 chain of both POPC and POPG. Overall, the presence of serotonin decreases the average chain order parameter by 3 to 19%. At 25 °C, 10 mol% serotonin does not alter the order parameter profile of POPC- d_{31} significantly. However, a drastic decrease in chain order is observed in the presence of 25 mol% serotonin. At 37 °C, the chain order decrease is identical for both serotonin concentrations. POPG- d_{31} responds more drastically to the presence of serotonin at both temperatures, but only minor differences are observed between the two serotonin concentrations probed here (shown in Figure 3A). The decrease in lipid chain order leads to a decrease in the average chain length of the lipids. These serotonin-induced lipid chain length alterations can be precisely calculated for both phospholipids of the mixture using the mean torque model.^[42] The average chain lengths of both POPC and POPG of the mixture in the absence and in the presence of serotonin is plotted in Figure 3B. Serotonin causes the lipid chains to decrease in length by ΔL , where ΔL is between 0.3 and 0.9 Å. This decrease in the lipid chain length is due to a serotonin-induced increase in the number of *gauche* conformers in the chains.

We then probe the average location of serotonin in POPC membranes using ^1H NOESY NMR. This technique is well-suited to localize a small lipophilic molecule in the membrane and to determine its distribution parallel to the membrane normal.^[43] However, the experiment has a much longer intrinsic timescale comparable to the ^1H spin-lattice relaxation time of lipids, which is on the order of 0.25 s. In this time, lipids typically visits an area with a radius of $\approx 1\ \mu\text{m}$ by diffusion.^[39] The cross-relaxation rates represent the contact probability between the individual protons of serotonin with the respective lipid segments.^[43] Our results show that the ring system of serotonin is broadly distributed within the membrane with a maximum found in the glycerol region, which is at the lipid-water interface of the membrane (Figure 3C–F). The molecular basis of the disordering effect of serotonin on lipid acyl chains can be understood from these results. Serotonin inserts into the lipid membrane and intercalates between neighboring lipid molecules in the glycerol region. This creates free volume in the acyl chain region of the membrane, which is occupied by larger amplitude motions of the chains, resulting in the observed lowering of the chain order parameters.^[27,28] The NMR

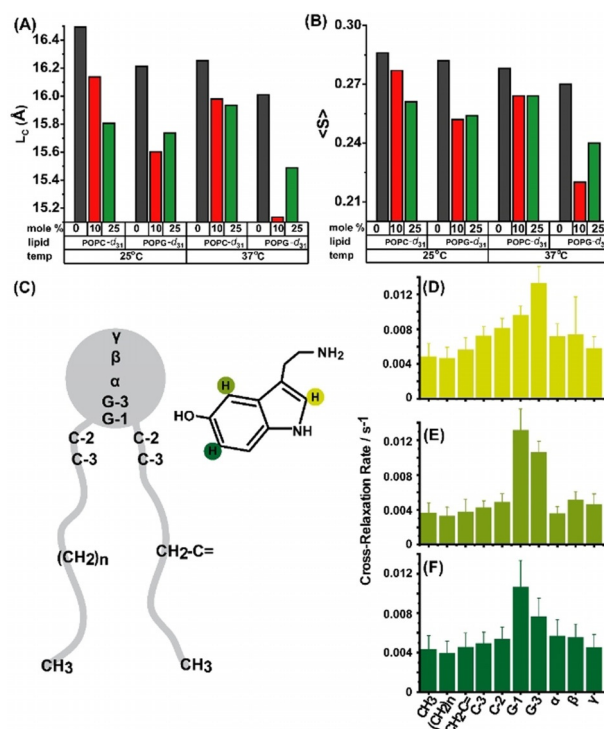


Figure 3. Probing the distribution and effect of serotonin in lipid bilayer by solid-state NMR. (A) Average lipid chain length of POPC- d_{31} :POPG:cholesterol (1:1:1) and POPC:POPG- d_{31} :cholesterol (1:1:1) with 0, 10, 25 mol% of serotonin at (i) 25 °C and (ii) 37 °C. (B) ^2H NMR average order parameters of the above mentioned membrane composition. (C) schematic representation of serotonin interaction with POPC lipid chain segment. (D,E,F) are the ^1H NOESY NMR cross-relaxation rates representing the contact probability between the individual protons of serotonin labelled in (C) with the respective lipid segments.

results corroborate the decrease in the force of indentation of the membranes observed by AFM. We note that this effect may depend on the nature of the lipid, since serotonin may distribute differently in bilayers of different compositions.^[17]

Effect of serotonin on cell membranes

Serotonin increases membrane binding of amyloid oligomers

We hypothesize that the observed alterations in the mechanical properties of the membrane may contribute to the action of serotonin on cells. An increase of membrane disorder may facilitate the binding of small extracellular molecules and peptides to the membrane, and this may have physiological consequences. Furthermore, membrane protein function is strongly related to the elastic properties of the bilayer,^[44,45] and lipids can allosterically regulate membrane protein activity.^[46] We probe the affinity of IAPP oligomers to the membrane of live cells in the presence of extracellular serotonin. IAPP is an amyloidogenic peptide that is co-secreted with serotonin from pancreatic beta cells, and its membrane interaction has been linked to type II diabetes.^[47–49] We have already shown that the oligomeric form of this peptide has a large membrane affinity, which may partly explain its biologically toxic role.^[50] It is plausible that membrane stiffness will affect the insertion of a pro-

tein, such as the IAPP oligomer. We therefore examine whether IAPP binding to the cell membrane and its uptake is modulated by serotonin. However, most mammalian cells have receptors for serotonin, so serotonin can, in principle, also modulate this process via a receptor-mediated pathway. Here we have used the RN46A cells, which is an immortalized serotonergic cell line derived from rat raphe nuclei.^[51]

With the help of polymerase chain reaction (PCR), we determine that the major serotonergic receptors present in the RN46A cells are the serotonin 5-HT_{1A} and 5-HT_{2C} (supplementary Figure S9). mRNA expression levels of other 5-HT receptors (5-HT_{1B}, 5-HT₃, 5-HT₄, and 5-HT₇ receptors) are not significant. To block 5-HT_{1A} and 5-HT_{2C} receptors, as well as the serotonin transporters (SERTs), we pre-treat the cells with WAY100635^[52] (10 μM), Methysergide (10 μM), Ketanserin^[53] (10 μM) and Fluoxetine (10 μM) in all cell experiments. The cells are then washed with fresh Thomson's buffer (TB) and incubated with 200 nM of rhodamine-labeled IAPP oligomers for 30 min. The cells are washed again with fresh TB and imaged in TB using a confocal microscope (Zeiss 880, Germany). The average fluorescence intensity of the cell region is analyzed after subtraction of the non-cell background, using ImageJ software,^[54] and reports the extent of IAPP binding. The results are depicted in Figure 4A and 4B. We see that IAPP binding increases by $32.0 \pm 10.6\%$ ($p < 0.05$) when the cells are incubated with 0.5 mM serotonin. We use a 10 times lower concentration of serotonin compared to the bilayer experiments, as we do not want to cause the large changes of membrane stiffness observed in those studies. Cells treated with just the blocking agents do not exhibit any change in intensity (supplementary Figure S10C). We note that serotonin also quenches rhodamine fluorescence. Therefore, the actual increase, which is measured by the increase of fluorescence at the membrane and inside the cell, is likely larger than the measured increase. Supporting Figure S11 describes a separate experiment which characterizes the quenching of PPC111 lipid membrane-bound Rh-IAPP by serotonin. The extent of quenching at the concentration level used in these biological experiments is 49%. So we estimate that the actual level of increase of IAPP binding can be 2.6 ± 0.3 times. Collectively these experiments show that serotonin binding can strongly alter the affinity of cell membranes to extracellular proteins and peptides.

Serotonin enhances endocytosis

We also probe whether serotonin modulation of the membrane properties affects the process of endocytosis. Endocytosis requires the generation of large membrane curvatures, which should be facilitated by the decrease of the membrane stiffness. So the rate of endocytosis may be expected to be enhanced by serotonin. We use a constitutive endocytosis process, not known to be related to serotonin signaling, as a measure for the modulation of cellular endocytosis rates. We follow the rate of endocytosis of the transferrin (Tf) receptor using a fluorescent transferrin conjugate (Alexa Fluor488-transferrin). The experiments are similar to those described for IAPP binding and are also performed in the presence of the sero-

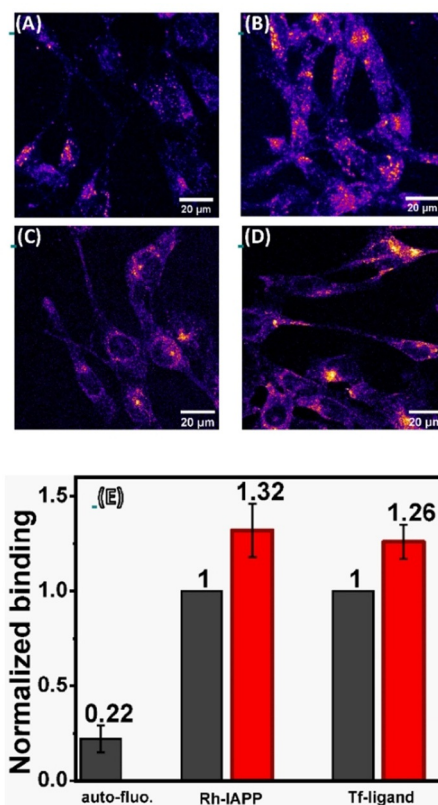


Figure 4. Effect of serotonin on the interaction of RN46A cells with amylin (IAPP) and transferrin. (A,B) Confocal images of the binding and internalization of Rhodamine (Rh)-labelled IAPP oligomers to RN46A cells in the absence (A) and in the presence (B) of serotonin. (C,D) Confocal images of transferrin receptor internalization by RN46A cells showing AlexaFluor488-transferrin distribution in absence (C) and in presence (D) of serotonin. (E) analysis of the extent of binding of different probes in absence (black) and in presence (red) of serotonin. Cells are pre-treated with 5-HT_{1A} receptor antagonist, WAY100635 (10 μM), 5-HT₂ receptor antagonists Methysergide (10 μM) and Ketanserin (10 μM), and SERT inhibitor Fluoxetine (10 μM).

nin transporter inhibitor (fluoxetine) and receptor antagonists (Way100635, methysergide, and ketanserin). The integrated brightness of the cell after 15 min of incubation with Alexa488-Tf is used as a measure of the rate of endocytosis. The images are recorded with a confocal microscope using 488 nm Argon laser excitation. The total intracellular intensity is calculated by z-projecting the image stacks and subsequently delineating the cell boundaries manually. We observe that the level of transferrin internalization goes up by a factor of $26.0\% \pm 7.1\%$ ($p < 0.05$) in the presence of serotonin, as shown in Figure 4C and D. This indicates that serotonin-membrane interaction can affect membrane proteins unrelated to serotonin, potentially providing a membrane-mediated pathway for modulating the physiological states of cells. However, we note that it is difficult to establish that alteration of membrane mechanics is the sole cause behind this observed effect.

Discussion

Serotonin is water-soluble up to > 2 M concentration, yet it attaches to lipid membranes with a partition coefficient of up to

1500. Vesicular membranes and plasma membranes near serotonin release sites are therefore expected to contain a considerable concentration of serotonin. Here we address whether this large amount of membrane-incorporated serotonin has any direct effect on the membrane properties. This question assumes significance because any change of membrane properties will likely affect fundamental cellular processes that are mediated by the membrane, such as *endo-* and *exocytosis*, local membrane organization, and dynamics of membrane proteins.

High membrane partitioning of serotonin has been reported in DMPC and DOPC vesicles.^[16] This also leads to a decrease in lipid chain order and a restructuring of the domain size in raft model mixtures.^[27,28] Here we show that high membrane partitioning is also true for multicomponent membranes containing zwitterionic (DEC221) and negatively charged lipids (PPC111), and also bilayers containing sphingomyelin and cholesterol (Figure S1). The molar serotonin-to-lipid ratio in vesicles exposed to 4.1 mM serotonin is 0.7% for the zwitterionic lipid vesicles, while it is 11% for the negatively charged vesicles. Thus, a substantial quantity of serotonin is present in the membrane, and depending on their location, they can be expected to have significant effects on membrane properties.

Two of the major properties of a membrane are its stiffness and local order. These parameters can influence the membrane traffic and also the functioning of membrane proteins, especially those molecules which undergo large conformational changes during their function. We measure the influence of serotonin on both of these properties. In principle, the effect of membrane insertion by a small molecule such as serotonin will depend on the nature of the headgroup, the type of alkyl chains present in the lipids, and the location of the molecule in the lipid bilayer. The negatively charged PPC111 membrane shows a profound lowering of the indentation force, going from an average of 2.5 ± 0.2 nN to 1.1 ± 0.1 nN (Figure 1C). The area of the interface between two domains is equal to the perimeter. The zwitterionic biphasic DEC221 bilayer also shows a decrease, but mostly in the stiffness of the ordered domains. Though Figure S2 shows that serotonin has higher affinity to the disordered domains, it still binds substantially to the ordered domain, and alters its properties. Significantly, serotonin decreases the area of the ordered domains (Figure 2), and nucleates disordered phases within the ordered ones. The surface tension at the interface between the two phases reduces by $34.0 \pm 2.1\%$, clearly indicating that serotonin has a strong effect on the ordered phase. We note that our measure of the surface tension is different from the line tension that can be obtained from the analysis of the indentation force distributions, which is a measure of the surface tension between the lipid and the aqueous phases.^[55,56] These cholesterol- and sphingomyelin-rich ordered domains are representative of raft-like structures on the cell membrane, which are important for cellular signaling processes.^[36,38,57,58] Serotonin-induced reduction of the fractional area of the ordered domain can, therefore, have significant consequences for cell signaling.

Molecules, such as cholesterol or anesthetics,^[2,32,59] can change membrane properties, depending on the location of

the molecule in the lipid bilayer. Molecular dynamic simulations suggest that serotonin primarily localizes in the upper half of each leaflet of the membrane.^[16,28] Our solid-state NMR spectroscopy results show that serotonin can be distributed throughout the membrane, but its average location is close to the glycerol group of the phospholipids. The order parameter measurement reveals that the disorder of the lipid chains indeed increases considerably (Figure 3), and the lipid chain effectively shortens by about 0.5 Å. These results are clearly in agreement with the increase of disorder observed in our AFM force measurements. Changes in membrane stiffness, local membrane heterogeneity and effective chain lengths of the lipids may transduce the presence of serotonin and modulate membrane traffic and protein binding, and also allosterically regulate membrane protein behavior. However, it is not straightforward to exclusively measure the membrane-mediated effects of serotonin. Most neurons, and indeed, most cell types in the human body have serotonin receptors,^[60] so the effects will be dominated by serotonin receptor-driven signaling. We determine the types of serotonin receptors present in the RN46A serotonergic neuronal cell line used for our study and carry out all our cellular measurements under adequate concentrations of antagonists for these serotonergic receptors (as well as the serotonin transporters). An increase in membrane disorder can be expected to facilitate the insertion of molecules with high membrane affinity. We observe that binding and uptake of IAPP oligomers (associated with type II diabetes) by the cells are indeed enhanced in the presence of 0.5 mM of serotonin (Figure 4A and B). It is interesting to note that serotonin is co-secreted by the pancreatic beta cells together with IAPP,^[49,61–63] so the effect of serotonin on the degree of membrane attachment of IAPP could be physiologically significant. A reduction in stiffness should also promote *exo-* and *endocytosis*, by allowing the formation of larger curvatures in the membrane. We investigate the effect of serotonin binding on the rate of *endocytosis* by measuring the internalization of transferrin receptors. The transferrin receptors have no known interactions with serotonin, yet we observe a considerable increase in their *endocytosis* in the presence of serotonin (Figure 4C,D). Thus two important membrane-mediated processes, that is, protein binding and the rate of *endocytosis*, are both strongly modulated by serotonin. This indicates that critical cellular processes may respond to serotonin via membrane-mediated effects, independent of the more traditional receptor-mediated signaling pathways.

It may be asked whether the concentrations of serotonin used in our experiments (4.1 mM for the studies on artificial bilayers, 0.5 mM for cell experiments) are physiologically relevant. The serotonergic vesicles are known to contain >250 mM of serotonin,^[64,65] much more than the concentrations used here. So the vesicular membrane will be saturated with serotonin, and during *exocytosis*, these will provide serotonin-rich membrane patches for mediating activity on the plasma membrane. However, a substantial amount of serotonin is also directly available to the plasma membrane, at least transiently, near the site of vesicular release. Model calculations suggest that the release of a single small monoaminergic synaptic vesicle

can elevate the extracellular concentration of monoamines to several μM for $\approx\text{ms}$ time scales.^[66] However, cell soma can perform a sustained release of hundreds of vesicles of much larger size (with diameters $> 100\text{ nm}$ compared to the $\approx 40\text{ nm}$ typical synaptic vesicles).^[64,65,67] Given that serotonin strongly partitions into the membrane, such sustained release may have a cumulative effect on the membrane serotonin availability. Therefore, a $\approx\text{mM}$ serotonin concentration may not be unusually high for the plasma membrane near the release sites. So the biophysical and cellular effects observed here may also be expected to occur *in vivo*.

Conclusion

Overall, our experiments show that serotonin, at concentration levels relevant *in vivo*, can interact with the cell membrane, increase membrane disorder, and profoundly change the membrane modulated properties of cells. The membrane provides a ubiquitously present effector for serotonin, through which it can directly influence cellular physiology, in keeping with other receptor-independent roles of serotonin such as serotonylation of target proteins.^[63,68] This membrane-mediated pathway may be secondary to the conventional receptor-mediated pathways, but it will be rather important in situations, for example, where those receptors are inhibited by pharmaceutical agents. Its influence on membrane processes can also become an important consideration when the extracellular serotonin is maintained at an elevated level by serotonin transporter blockers. Therefore, a comprehensive understanding of serotonin biology and pharmacology needs to take this novel membrane-mediated pathway into account.

Experimental Section

Materials and Methods

Materials: The lipids 1-palmitoyl-2-oleoyl-*sn*-glycero-3-phosphocholine (POPC), 1-palmitoyl-2-oleoyl-*sn*-glycero-3-phospho-*rac*-(1'-glycerol) (POPG), 1,2-dioleoyl-*sn*-glycero-3-phosphocholine (DOPC), *N*-hexadecanoyl-*D*-erythro-sphingosylphosphorylcholine (egg SM) as well as the in the *sn*-1 chain per-deuterated versions POPC-*d*₃₁ and POPG-*d*₃₁ were purchased as powder from Avanti Polar Lipids (Alabaster, AL), cholesterol and *ortho*-phthalaldehyde (OPA), Way100635 maleate, Methysergide maleate and Ketanserin tartrate were purchased from Sigma (St. Louis, MO). Serotonin-hydrochloride was purchased from Merck (Darmstadt, Germany). Chloroform and methanol AR graded were purchased from S. D. Fine-Chemicals Ltd. (India), and Milli-Q water (Millipore, Merck), deionized to a resistivity of $18.2\text{ M}\Omega\cdot\text{cm}^{-1}$, were used for all experiments. Lipid extruding kit and Nucleopore Track-etched polycarbonate membrane of 50 nm pore diameter were bought from Avanti Polar Lipids (Alabaster, AL). Biotech CE Tubing: 100 kDa MWCO dialysis membrane was purchased from Spectrum Laboratories, Inc. (MA, USA). Fluoxetine hydrochloride was purchased from Tocris Bioscience (Minneapolis, MN). Alexa Fluor488-transferrin was purchased from Molecular Probes (Eugene, OR).

Preparation of planar supported lipid bilayers: Planar supported lipid bilayers were prepared by the vesicle fusion method.^[69] To prepare POPC/POPG/cholesterol in 1/1/1 molar ratio (PPC111), the

required amount of lipids was dissolved in chloroform. For DOPC/egg SM/cholesterol in 2/2/1 molar ratio (DEC221), the required amount of lipids was dissolved in 1:1 (by volume) methanol:chloroform. The solvent was evaporated under a flux of extra pure Argon and then subjected to a vacuum for 24 hours for complete removal of organic solvents. The lipid films were rehydrated in water to a final concentration of 2.5 mg mL^{-1} . The lipid suspension was then vortexed vigorously and extruded using 50 nm pore diameter polycarbonate membrane at 60°C . After extrusion, $40\text{ }\mu\text{L}$ of $100\text{ mM CaCl}_2 \cdot 2\text{H}_2\text{O}$, $50\text{ }\mu\text{L}$ of extruded lipid solution and $210\text{ }\mu\text{L}$ of Milli-Q water were deposited sequentially on freshly cleaved mica previously glued on to a glass coverslip affixed to a liquid incubated for 1 h at 60°C in a water bath and slowly cooled down to room temperature. The samples were rinsed extensively with deionized water to remove non-fused vesicles. The presence of bilayers was confirmed using AFM. AFM contact mode imaging shows that the ternary mixture containing DOPC, egg SM, and cholesterol (2:2:1) forms a continuous biphasic bilayer with $\approx 1\text{ nm}$ height difference between the two phases. The PPC111 bilayer has no phase separation and no image contrast. However, force indentation by AFM confirms the presence of the bilayer in the sample.

AFM imaging and force indentation: All AFM measurements were carried out using the NanoWizard II system (JPK Instruments, Berlin, Germany) which is mounted on an Axiovert Inverted Microscope (Zeiss, Germany). AFM topographic images were obtained in contact mode, using silicon nitride cantilevers (Bruker, Camarillo, CA) with a nominal spring constant of 0.01 N m^{-1} and a tip radius of 20 nm . The force during imaging was kept as low as possible, and the scan rate was kept at 1 Hz . Height, vertical and lateral deflection error signals were simultaneously recorded for both trace and retrace. All the AFM images were analyzed using JPK image processing software, and the images were plane fitted with a 1st order polynomial.

Force measurement was performed after the calibration of sensitivity, resonance frequencies (both in air and in water), and the spring constant, using the thermal noise method.^[70] The cantilever used for all force experiments has a resonance frequency of $10\text{--}20\text{ kHz}$ and a spring constant of 0.03 N m^{-1} . Sensitivity and spring constant measurements were performed after each experiment. The sensitivity values before and after the experiments remained the same within errors. All the AFM experiments were performed on mica glued to coverslip glass in a liquid cell. The bilayer was hydrated until the end of the experiment. The force indentation experiments on phase-separated DEC221 bilayers were preceded by imaging of the bilayer, which located the L_o and L_d domains. The indentation forces were measured then by selecting a small area inside both the L_o and L_d domains. For the PPC111 bilayer, the total Z piezo displacement was $1.0\text{ }\mu\text{m}$. The piezo velocity both for approach and retraction was kept at $0.5\text{ }\mu\text{m s}^{-1}$. For the DEC221 bilayer, the total Z piezo displacement was kept at $5.85\text{ }\mu\text{m}$. The piezo velocity both for approach and retraction was kept at $2.0\text{ }\mu\text{m s}^{-1}$. In the non-contact region, the AFM tip first approaches the top surface of the bilayer during which the force remains constant. As it hit the bilayer surface at the contact point, the force increases. At some point, the tip started indenting the bilayer, which was followed by a sudden breakthrough, which appeared as a 'kink' in the smooth approaching force-distance curve (shown in Figure 1A). This force is known as the indentation force. It was followed by the tip reaching the solid mica support. All the experiments were carried out at different positions on both DEC221 and PPC111 bilayer under similar conditions. The images and batches of indentation force curves were analyzed using JPK Data Processing software. Forces of in-

dentation were extracted from each approach curve to build the histogram.

Solid-state NMR spectroscopy: Lipids and serotonin, dissolved in organic solvents, were mixed and evaporated at 40 °C in a rotary evaporator. The molar ratios of all components were POPC/POPG/cholesterol/serotonin 1/1/1/0; 3/3/3/1 or 1/1/1/1 for ^2H NMR, and POPC/serotonin 3/1 for ^1H NOESY NMR measurements. After evaporation of the solvent, samples were re-dissolved in cyclohexane and converted into a fluffy powder by lyophilization overnight at high vacuum. The samples were hydrated with 50%wt K_2PO_4 buffer (20 mM K_2PO_4 , 100 mM NaCl, 0.1 mM EGTA pH 7.4) in Milli-Q water (^2H NMR) or D_2O (^1H NOESY NMR). After hydration, samples were freeze-thawed 10 times with gentle centrifugation for equilibration and finally transferred to 5 mm glass vials (^2H NMR) and 4 mm NMR rotors (^1H NOESY NMR).

^2H NMR measurements were acquired on a Bruker 750 NMR Avance I spectrometer (Bruker Biospin GmbH, Rheinstetten, Germany) at a resonance frequency of 115.1 MHz for ^2H . The two $\pi/2$ pulses were 2.35–2.5 μs , the relaxations delay 1 s, and the delay between the pulses 30 μs . A single-channel solids probe equipped with a 5 mm solenoid coil was used. The Pake doublets in the ^2H NMR spectra were assigned assuming a continuous order decrease from the glycerol towards the acyl chain ends. Order parameter profiles were calculated after de-Pakeing the spectra according to Huster et al.^[39] and projected chain length was calculated according to the mean torque model.^[42]

For the ^1H MAS NMR measurements, a Bruker Avance III 600 MHz NMR spectrometer equipped with a 4 mm high resolution MAS probe was used. The $\pi/2$ pulse length was 4 μs and 6 kHz was used as MAS frequency. ^2H lock was used for field stability. The chemical shift of the methyl group was calibrated relative to TMS at 0.885 ppm for the ^1H NMR spectra calibration. ^1H MAS NOESY NMR spectra using five mixing times of 0.1, 100, 200, 300, and 500 ms were acquired. The Bruker Topspin software 4 was used for assigning and integrating the volumes of the diagonal and cross peaks. Nonlinear regression curve fitter in Origin 2015 (OriginLab Cooperation, Northampton, MA, U.S.A.) was used to fit the experimental cross peaks at the different mixing times. From the fit the cross-relaxation times could be calculated, according to the spin-pair model.^[43]

Cell culture: RN46A cells (a rat serotonergic neuronal cell line) were cultured in Dulbecco's modified Eagle's media-F12 (1:1) (Gibco, USA) media supplemented with 10% heat-inactivated fetal bovine serum (Gibco, USA), 50 units mL^{-1} Penicillin and 50 $\mu\text{g mL}^{-1}$ Streptomycin (HiMedia, India) in T-25 canted neck flasks. Cultures were maintained in a humidified atmosphere at 37 °C with 5% CO_2 . Media were changed every 48 hours. For confocal imaging experiments, the cells were plated on poly-L-lysine (Sigma, St. Louis, MO, 0.1 mg mL^{-1}) coated coverslips and used the following day. Cells were imaged in Thomson's buffer (TB, consisting of 20 mM sodium HEPES, 146 mM NaCl, 5.4 mM KCl, 1.8 mM CaCl_2 , 0.8 mM MgSO_4 , 0.4 mM KH_2PO_4 , 0.3 mM Na_2HPO_4 , and 5 mM D-glucose; pH adjusted to 7.4).

Quantitative real-time polymerase chain reaction (qPCR) analysis: RNA was extracted from RN46A cells using the commercially available Trizol reagent (Invitrogen, USA). 2 μg of RNA was reverse transcribed to complementary DNA (cDNA), using a cDNA synthesis kit (PrimeScript 1st strand cDNA Synthesis Kit, Takara Bio), according to the manufacturer's instructions. cDNA was then diluted and subjected to quantitative real-time PCR, using gene-specific primers and KAPA SYBR (KAPA Biosystems), on a Bio-Rad CFX96 real-time PCR machine. 18S ribosomal RNA was used as a house-keeping gene to normalize gene expression levels, and relative ex-

pression levels were calculated by the DDCT method, as described previously.^[71]

Confocal microscopy: Confocal fluorescence microscopy on both bilayers and RN46A cells was performed on LSM 880 (Zeiss, Germany). For confocal imaging of bilayers and RN46A, 488 nm and 543 nm, 633 nm excitation light were taken from Ar⁺⁺ and He-Ne laser, respectively, which were reflected by a dichroic mirror (MBS 488/543/633) and focused through a Zeiss C-Apochromat 40x, NA 1.2, water immersion objective onto the sample. The fluorescence emission was collected by the same objective and sent to a GaAsP detector.

Acknowledgements

SM acknowledges support of the Department of Atomic Energy, Government of India, provided under project no. RTI4003. DH acknowledges funding by the Deutsche Forschungsgemeinschaft (DFG, German Research Foundation) through SFB 1423, project number 421152132, subproject A02. OE and also acknowledges support by the Sigrid Juselius Foundation, and Ruth and Nils-Erik Stenbäck's Foundation. Open access funding enabled and organized by Projekt DEAL.

Conflict of interest

The authors declare no conflict of interest.

Keywords: lipid bilayers • membrane modulation • neurotransmission • serotonin-membrane interaction • volume transmission

- [1] E. R. Kandel, T. M. Jessell, S. Siegelbaum, *Principles of Neural Science* McGraw-Hill, New York, 2021.
- [2] R. S. Cantor, *Biochemistry* 2003, 42, 11891–11897.
- [3] A. L. Revill, N. Y. Chu, L. Ma, M. J. LeBlancq, C. T. Dickson, G. D. Funk, *J. Physiol.* 2019, 597, 3183–3201.
- [4] F. Saitow, M. Murano, H. Suzuki, *J. Neurophysiol.* 2009, 101, 1361–1374.
- [5] M. Murano, F. Saitow, H. Suzuki, *Neuroscience* 2011, 172, 118–128.
- [6] J. C. Strahlendorf, M. Lee, H. K. Strahlendorf, *Neuroscience* 1989, 30, 117–125.
- [7] C. Trueta, F. De-Miguel, *Front. Physiol.* 2012, 3, 319.
- [8] L. F. Agnati, M. Zoli, I. Strömberg, K. Fuxe, *Neuroscience* 1995, 69, 711–726.
- [9] M. A. Bunin, R. M. Wightman, *J. Neurosci.* 1998, 18, 4854–4860.
- [10] F. F. De-Miguel, C. Trueta, *Cell. Mol. Neurobiol.* 2005, 25, 297–312.
- [11] S. K. Kaushalya, R. Desai, S. Arumugam, H. Ghosh, J. Balaji, S. Maiti, *J. Neurosci. Res.* 2008, 86, 3469–3480.
- [12] F. F. De-Miguel, C. Leon-Pinzon, P. Noguez, B. Mendez, *Philos. Trans. R. Soc. London Ser. B* 2015, 370, 20140196.
- [13] E. Quentin, A. Belmer, L. Maroteaux, *Front. Neurosci.* 2018, 12, 982.
- [14] E. Del-Bel, F. F. De-Miguel, *Front. Synaptic Neurosci.* 2018, 10, 13.
- [15] K. Fuxe, A. Dahlström, M. Höistad, D. Marcellino, A. Jansson, A. Rivera, Z. Diaz-Cabiale, K. Jacobsen, B. Tinner-Staines, B. Hagman, G. Leo, W. Staines, D. Guidolin, J. Kehr, S. Genedani, N. Belluardo, L. F. Agnati, *Brain Res. Rev.* 2007, 55, 17–54.
- [16] G. H. Peters, C. Wang, N. Cruys-Bagger, G. F. Velardez, J. J. Madsen, P. Westh, *J. Am. Chem. Soc.* 2013, 135, 2164–2171.
- [17] B. P. Josey, F. Heinrich, V. Silin, M. Lösche, *Biophys. J.* 2020, 118, 1044–1057.
- [18] P. A. Postila, I. Vattulainen, T. Róg, *Sci. Rep.* 2016, 6, 19345.
- [19] P. A. Postila, T. Róg, *Mol. Neurobiol.* 2020, 57, 910–925.
- [20] S. Chakraborty, M. Doktorova, T. R. Molugu, F. A. Heberle, H. L. Scott, B. Dzikovski, M. Nagao, L.-R. Stingaciu, R. F. Standaert, F. N. Barrera, J. Kat-

- saras, G. Khelashvili, M. F. Brown, R. Ashkar, *Proc. Natl. Acad. Sci. USA* **2020**, *117*, 21896–21905.
- [21] H. Tsuchiya, M. Mizogami, *Anesthesiol. Res. Prac.* **2013**, 297141.
- [22] R. Kapoor, T. A. Peyear, R. E. Koeppel II, O. S. Andersen, *J. Gen. Physiol.* **2019**, *151*, 342–356.
- [23] H. M. Seeger, M. L. Gudmundsson, T. Heimburg, *J. Phys. Chem. B* **2007**, *111*, 13858–13866.
- [24] S. Schreier, S. V. P. Malheiros, E. de Paula, *Biochim. Biophys. Acta* **2000**, *1508*, 210–234.
- [25] E. I. I. Eger, D. E. Raines, S. L. Shafer, H. C. J. Hemmings, J. M. Sonner, *Anesth. Analg.* **2008**, *107*, 832–848.
- [26] M. Robinson, S. Turnbull, B. Y. Lee, Z. Leonenko, *Biochim. Biophys. Acta* **2020**, *1862*, 183363.
- [27] O. Engberg, A. Bocicchio, A. F. Brandner, A. Gupta, S. Dey, S. Maiti, R. A. Böckmann, D. Huster, *Front. Physiol.* **2020**, *11*, 578868.
- [28] A. Bocicchio, A. F. Brandner, O. Engberg, D. Huster, R. Böckmann, *Front. Cell. Dev. Biol.* **2020**, *8*, 601145.
- [29] D. Bhowmik, A. K. Das, S. Maiti, *Langmuir* **2015**, *31*, 4049–4053.
- [30] S. Maiti, J. B. Shear, R. M. Williams, W. R. Zipfel, W. W. Webb, *Science* **1997**, *275*, 530–532.
- [31] K. Bera, A. K. Das, A. Rakshit, B. Sarkar, A. Rawat, B. K. Maity, S. Maiti, *ACS Chem. Neurosci.* **2018**, *9*, 469–474.
- [32] R. M. A. Sullan, J. K. Li, C. Hao, G. C. Walker, S. Zou, *Biophys. J.* **2010**, *99*, 507–516.
- [33] a) N. Kahya, D. Scherfeld, K. Bacia, B. Poolman, P. Schwille, *J. Biol. Chem.* **2003**, *278*, 28109–28115; b) A. Bunge, P. Müller, M. Stöckl, A. Herrmann, D. Huster, *Biophys. J.* **2008**, *94*, 2680–2690.
- [34] M. M. Lozano, J. S. Hovis, F. R. Moss 3rd, S. G. Boxer, *J. Am. Chem. Soc.* **2016**, *138*, 9996–10001.
- [35] S. Ip, J. K. Li, G. C. Walker, *Langmuir* **2010**, *26*, 11060–11070.
- [36] K. Simons, E. Ikonen, *Nature* **1997**, *387*, 569–572.
- [37] J. P. Slotte, *Prog. Lipid Res.* **2013**, *52*, 424–437.
- [38] V. A. Villar, S. Cuevas, X. Zheng, P. A. Jose, *Methods Cell Biol.* **2016**, *132*, 3–23.
- [39] D. Huster, K. Arnold, K. Gawrisch, *Biochemistry* **1998**, *37*, 17299–17308.
- [40] M. F. Brown, *J. Magn. Reson.* **1979**, *35*, 203–215.
- [41] J. H. Davis, *Biochim. Biophys. Acta* **1983**, *737*, 117–171.
- [42] H. I. Petrasche, S. W. Dodd, M. F. Brown, *Biophys. J.* **2000**, *79*, 3172–3192.
- [43] H. A. Scheidt, D. Huster, *Acta Pharmacol. Sin.* **2008**, *29*, 35–49.
- [44] M. F. Brown, *Chem. Phys. Lipids* **1994**, *73*, 159–180.
- [45] M. F. Brown, *Curr. Top. Membr.* **1997**, *44*, 285–356.
- [46] R. Dawaliby, C. Trubbia, C. Delporte, M. Masureel, P. Van Antwerpen, B. K. Kobilka, C. Govaerts, *Nat. Chem. Biol.* **2016**, *12*, 35–39.
- [47] S. E. Kahn, S. Andrikopoulos, C. B. Verchere, *Diabetes* **1999**, *48*, 241–253.
- [48] S. Trikha, A. M. Jeremic, *J. Biol. Chem.* **2011**, *286*, 36086–36097.
- [49] J. Almaça, J. Molina, D. Menegaz, A. N. Pronin, A. Tamayo, V. Slepak, P.-O. Berggren, A. Caicedo, *Cell Rep.* **2016**, *17*, 3281–3291.
- [50] A. Rawat, B. K. Maity, B. Chandra, S. Maiti, *Biochim. Biophys. Acta* **2018**, *1860*, 1734–1740.
- [51] L. White, M. Eaton, M. Castro, K. Klose, M. Globus, G. Shaw, S. Whittemore, *J. Neurosci.* **1994**, *14*, 6744–6753.
- [52] S. T. Szabo, C. de Montigny, P. Blier, *Int. J. Neuropsychopharmacol.* **2000**, *3*, 1–11.
- [53] J. A. Dormandy, A. Berent, S. J. M. Downes, *Eur. J. Vasc. Surg.* **1988**, *2*, 371–375.
- [54] J. Schindelin, I. Arganda-Carreras, E. Frise, V. Kaynig, M. Longair, T. Pietzsch, S. Preibisch, C. Rueden, S. Saalfeld, B. Schmid, J.-Y. Tinevez, D. J. White, V. Hartenstein, K. Eliceiri, P. Tomancak, A. Cardona, *Nat. Methods* **2012**, *9*, 676–682.
- [55] H.-J. Butt, V. Franz, *Phys. Rev. E* **2002**, *66*, 031601.
- [56] R. M. A. Sullan, W. Shi, H. Chan, J. K. Li, G. C. Walker, *Soft Matter* **2013**, *9*, 6245–6253.
- [57] D. A. Brown, E. London, *Annu. Rev. Cell Dev. Biol.* **1998**, *14*, 111–136.
- [58] D. A. Brown, E. London, *J. Biol. Chem.* **2000**, *275*, 17221–17224.
- [59] a) N. Weizenmann, D. Huster, H. A. Scheidt, *Biochim. Biophys. Acta* **2012**, *1818*, 3010–3018; b) L. E. Nikitina, R. S. Pavelyev, V. A. Startseva, S. V. Kiselev, L. F. Galiullina, O. V. Aganova, A. F. Timerova, S. V. Boichuk, Z. R. Azizova, V. V. Klochkov, D. Huster, I. A. Khodov, H. A. Scheidt, *J. Mol. Liq.* **2020**, *301*, 112366; c) L. Galiullina, H. A. Scheidt, D. Huster, A. Aganov, V. Klochkov, *Biochim. Biophys. Acta* **2019**, *1861*, 584–593; d) J. Kremkow, M. Luck, D. Huster, P. Müller, H. A. Scheidt, *Biomolecules* **2020**, *10*, E1384.
- [60] J. Masson, M. B. Emerit, M. Hamon, M. Darmon, *WIREs Membr. Transp. Signal.* **2012**, *1*, 685–713.
- [61] G. Erik, *J. Endocrinol.* **1978**, *78*, 239–248.
- [62] L. D'Este, S. J. Wimalawansa, T. G. Renda, *Arch. Histol. Cytol.* **1995**, *58*, 537–547.
- [63] N. Paulmann, M. Grohmann, J.-P. Voigt, B. Bert, J. Vowinkel, M. Bader, M. Skelin, M. Jevsek, H. Fink, M. Rupnik, D. J. Walther, *PLoS Biol.* **2009**, *7*, e1000229.
- [64] D. Bruns, R. Jahn, *Nature* **1995**, *377*, 62–65.
- [65] J. Balaji, R. Desai, S. K. Kaushalya, M. J. Eaton, S. Maiti, *J. Neurochem.* **2005**, *95*, 1217–1226.
- [66] M. E. Rice, S. J. Cragg, *Brain Res. Rev.* **2008**, *58*, 303–313.
- [67] D. Bruns, D. Riedel, J. Klingauf, R. Jahn, *Neuron* **2000**, *28*, 205–220.
- [68] D. J. Walther, J. U. Peter, S. Winter, M. Höltje, N. Paulmann, M. Grohmann, J. Vowinkel, V. Alamo-Bethencourt, C. S. Wilhelm, G. Ahnert-Hilger, M. Bader, *Cell* **2003**, *115*, 851–862.
- [69] H. M. McConnell, T. H. Watts, R. M. Weis, A. A. Brian, *Biochim. Biophys. Acta* **1986**, *864*, 95–106.
- [70] J. L. Hutter, J. Bechhoefer, *Rev. Sci. Instrum.* **1993**, *64*, 1868–1873.
- [71] T. D. Schmittgen, K. J. Livak, *Nat. Protoc.* **2008**, *3*, 1101–1108.

Manuscript received: January 27, 2021

Accepted manuscript online: January 27, 2021

Version of record online: March 12, 2021